


Article

Catalytic Hydrocracking of Fresh and Waste Frying Oil over Ni- and Mo-Based Catalysts Supported on Sulfated Silica for Biogasoline Production

Karna Wijaya ^{1,*}, Asma Nadia ¹, Arina Dinana ¹, Amalia Febia Pratiwi ¹, Alfrets Daniel Tikoalu ² and Arief Cahyo Wibowo ³ 

- ¹ Department of Chemistry, Faculty of Mathematics and Natural Sciences, Universitas Gadjah Mada, Yogyakarta 55281, Indonesia; asmanadia@mail.ugm.ac.id (A.N.); arina.dinana.16@mail.ugm.ac.id (A.D.); amaliafeb99@mail.ugm.ac.id (A.F.P.)
- ² Institute for Nanoscale Science and Technology, Flinders University, Bedford Park, Adelaide 5042, Australia; alfrets.tikoalu@flinders.edu.au
- ³ Department of Applied Sciences, College of Arts and Sciences, Abu Dhabi University, Abu Dhabi 59911, United Arab Emirates; arief.wibowo@adu.ac.ae
- * Correspondence: karnawijaya@ugm.ac.id

Abstract: The synthesis of a sulfated silica catalyst and its modification with Ni and/or Mo metal, along with its application for the hydrocracking of fresh and waste frying oil into biogasoline, were conducted. Synthesis of the catalysts was initiated with the sulfation of silica (SiO₂) material by H₂SO₄ using the sol-gel method. Ni and/or Mo metal were impregnated into the SO₄/SiO₂ matrix with concentration variations of 1, 2, and 3 wt%. The sulfation process and promotion by Molybdenum (Mo) metal in the modified catalyst successfully increased the catalytic activity and selectivity. Among the catalysts investigated, Ni-SS2 exhibited the best performance for the hydrocracking reaction with waste frying oil. This catalyst was able to achieve a conversion of the liquid product of 71.47% and a selectivity of 58.73% for the gasoline fraction (C₅-C₁₂). NiMo-SS3 showed the highest percentage of activity and selectivity in the hydrocracking of fresh frying oil at 51.50 and 43.22 wt%, respectively.

Keywords: hydrocracking; Ni; Mo; sulfated silica; fresh frying oil; waste frying oil



Citation: Wijaya, K.; Nadia, A.; Dinana, A.; Pratiwi, A.F.; Tikoalu, A.D.; Wibowo, A.C. Catalytic Hydrocracking of Fresh and Waste Frying Oil over Ni- and Mo-Based Catalysts Supported on Sulfated Silica for Biogasoline Production. *Catalysts* **2021**, *11*, 1150. <https://doi.org/10.3390/catal11101150>

Academic Editors: Alessandra Palella and Lorenzo Spadaro

Received: 10 September 2021
Accepted: 22 September 2021
Published: 25 September 2021

Publisher's Note: MDPI stays neutral with regard to jurisdictional claims in published maps and institutional affiliations.



Copyright: © 2021 by the authors. Licensee MDPI, Basel, Switzerland. This article is an open access article distributed under the terms and conditions of the Creative Commons Attribution (CC BY) license (<https://creativecommons.org/licenses/by/4.0/>).

1. Introduction

Over the past decade, many researchers have concentrated their efforts on developing biofuels from alternative and renewable sources to decrease the dependency on transportation fuels derived from fossil fuels. Biofuels have the potential to contribute toward meeting transportation fuel demand as an alternative fuel. Biofuel can be produced through a thermal and catalytic hydrocracking process. Hydrocracking is a process to convert larger hydrocarbon molecules into smaller molecules by simultaneous or sequential carbon bond breaking and hydrogenation [1]. In the catalytic hydrocracking process, a catalyst is needed. The catalyst serves to speed up the hydrocracking process. Catalysts that can be used for the hydrocracking process include heterogeneous catalysts impregnated with metals. The acid function of these catalysts originates from the impregnated materials, whilst the hydrogenation function derives from the metals [2]. These catalysts have been selected due to their outstanding activity, selectivity, and stability [3]. The commonly-used supports for such catalysts are metal oxides. Metal oxides are widely used as a catalyst support, or as a catalyst itself [4–6], in which silica (SiO₂) is included.

Silica is a polymer of silicic acid consisting of SiO₄ units which are tetrahedrally linked, with the general formula SiO₂ [7]. Silica has several advantages as a carrier, such as having a high surface area, good thermal and mechanical stability, high uniformity of pore distribution, high adsorption capacity, and regular pore networks for the diffusion

of the substrates and the reaction products [8,9]. Silica catalysts can be synthesized by the sol-gel method [10]. The sol-gel method has been shown to have several advantages, including excellent control over precursor solution stoichiometry, ease of composition modification, operation at relatively low temperatures, and the use of inexpensive and simple equipment [11].

The acidic nature of the catalyst is one of the determining factors for the success of the hydrocracking process [1,12]. A catalyst with a higher total acidity usually provides a higher catalytic performance in the hydrocracking process [13]. Sulfated silica (SO_4/SiO_2) is produced by the modification of silica in the presence of sulfuric acid. Sulfated silica (SO_4/SiO_2) synthesized using the sol-gel method can provide an acid catalyst with a large surface area [14]. The sulfated catalyst is also inexpensive and relatively stable when used in many organic reactions [15]. The sulfate ion (SO_4^{2-}) is a strong complexing agent compared to chloride and nitrate ions. Thus, if silica is modified with sulfate ions, a distinct catalyst product could be achieved compared to the use of other anions [16]. The SO_4^{2-} ions can act as ligands that donate lone pair electrons through the oxygen atoms, thus forming coordination bonds with the Si^{4+} cations as the central atoms [17].

Sulfated silica (SO_4/SiO_2) is known to have high acidity, but it is less resistant to deactivation. Thus, modification of the catalyst is necessary, which can be performed through the impregnation of transition metals. Fundamentally, transition metals can be used directly as catalysts, but their surface areas are relatively small; if they are used directly as catalysts, metal agglomeration will occur [18]. The transition metals that can be used to impregnate the matrix of a catalyst include nickel (Ni) and molybdenum (Mo). A previous study has shown that Ni and Mo successfully increased catalytic activity and selectivity compared to that achieved by thermal reaction [19,20]. Even though there are several studies addressing the catalytic performance of a variety of heterogenous solid acid catalysts for the hydrocracking process, to the best of our knowledge, the use of Ni and Mo impregnated on sulfated silica for biogasoline fraction ($\text{C}_5\text{-C}_{12}$) has not yet been reported. The present study focuses on the synthesis and characterization of Ni and/or Mo on sulfated silica, and its application in the hydrocracking of fresh and waste frying oil into the gasoline fraction ($\text{C}_5\text{-C}_{12}$).

2. Results

2.1. Fourier Transform Infrared Spectroscopy (FTIR) Analysis

The FTIR spectra for all catalysts (catalysts labeling refer to Materials and Methods section) are shown in Figure 1. Based on the FTIR spectra, there was a broadened peak in the range $3600\text{-}3000\text{ cm}^{-1}$ which corresponds to the stretching vibration of the -OH group from Si-OH [21,22]. The bending vibration of the -OH group of the Si-OH group appeared at about 1600 cm^{-1} [23].

The symmetrical stretching vibration of the Si-O group appeared at about 800 cm^{-1} . The peak around 1100 cm^{-1} was assigned to the asymmetric stretching vibration of the Si-O group, which partially overlaps with the stretching vibration of the S-OH group originating from the HSO_4^- ion [23]. The bending vibration of the Si-O group was shown at 470 cm^{-1} [24]. The inclusion of metal in the catalyst system did not change the absorption band significantly, indicating that the interaction between the metal and the SS matrix did not occur covalently, but rather electrostatically.

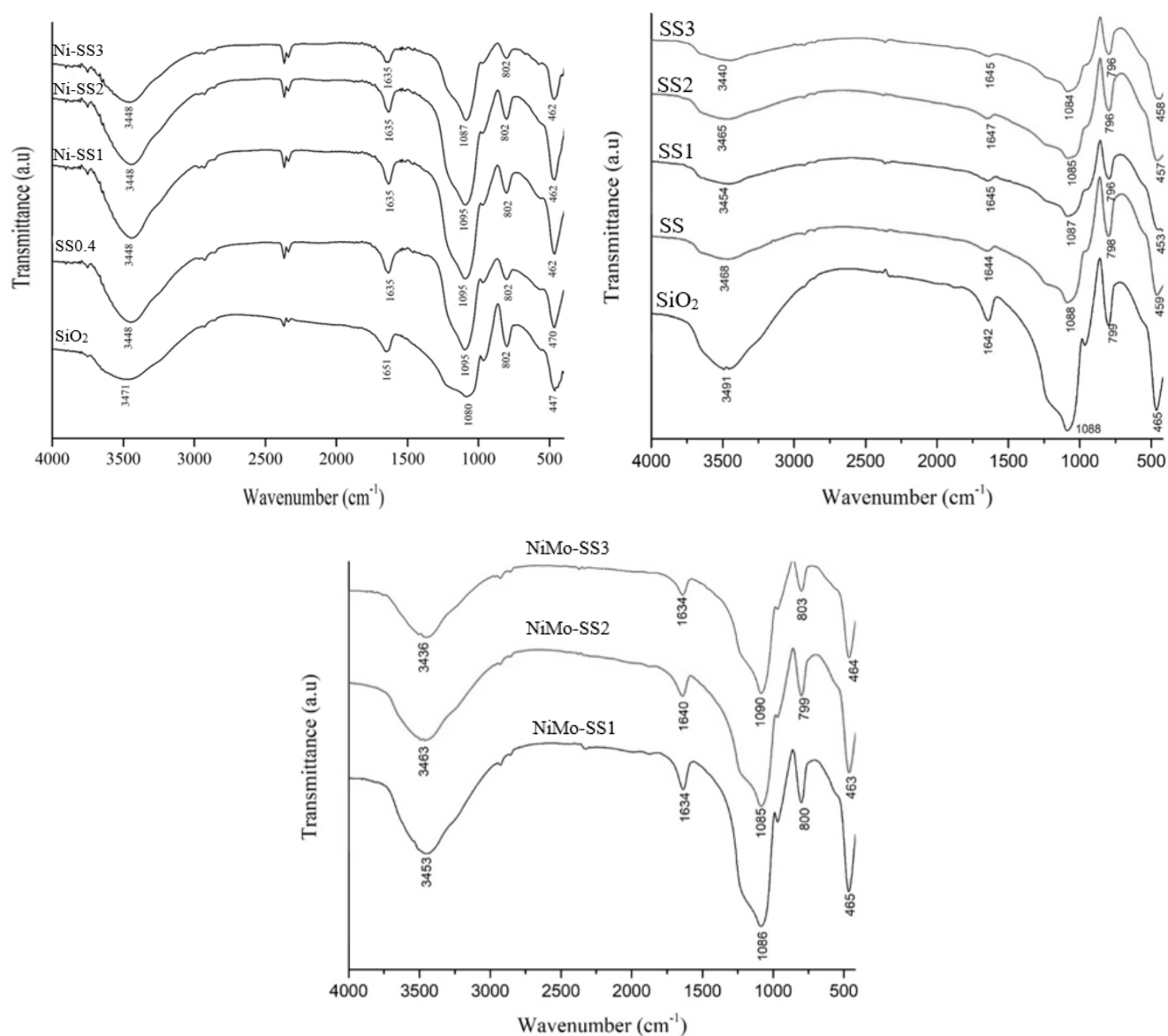


Figure 1. FTIR of all catalysts.

2.2. Total Acidity of Catalyst

The acidity test of the catalysts was carried out gravimetrically using the pyridine and ammonia adsorption technique [25,26]. The number of acid sites, with respect to pyridine as the basic adsorbate, is the number of the surface acid sites, assuming that the size of the pyridine molecules is relatively large so that it can only interact with the surface of the catalyst. The total number of acid sites in the models is equivalent to the amount of ammonia absorbed, due to its small size compared to pyridine molecules. The data from the catalyst acidity test is shown in Table 1. Based on Table 1, for the Ni/SS catalyst, there was an increase in the acidity due to the sulfation treatment. The acidity of the SiO₂ catalyst was initially 1.62 mmol/g, which is assumed to reflect the Lewis acid sites of the Si⁴⁺ ions that provide empty orbitals to bind with the pyridine base. The SS0.4 catalyst had an acidity value of 1.78 mmol/g. The increase in the acidity value was due to the presence of sulfate groups that entered the SiO₂ catalyst framework.

Table 1. Total acidity of the catalysts using pyridine.

Sample	Total Acidity (Ammonia-mmol/g)	Sample	Total Acidity (Pyridine-mmol/g)
NiMo/SS catalyst		Ni/SS Catalyst	
SiO ₂	6.03	SiO ₂	1.62
SS1	6.85	SS0.4	1.78
SS2	10.33	Ni-SS1	1.51
SS3	5.98	Ni-SS2	1.41
SS4	4.81	Ni-SS3	1.36
NiMo-SS1	13.41	-	-
NiMo-SS2	15.01	-	-
NiMo-SS3	15.70	-	-

In contrast, for the NiMo/SS preparation, the SS3 and SS4 catalysts underwent a decrease in their acidity. According to Ahmed et al. [27], the distribution and amount of sulfate on a matrix that has reached its maximum point will decrease the adsorbed base. The SS catalyst which had the highest acidity value was SS2, at 10.33 mmol/g.

Table 1 shows that the presence of Ni and/ or Mo on sulfated silica increased the total acidity. The total acidity was expected to increase as the metal concentration increased. Ni or Mo loaded onto the SS increases the acid amount significantly. It was observed that NiMo-SS3 had the highest total acidity at 15.70 mmol/g. However, the Ni/SS catalysts did not follow the same trend. There was an overall decrease in the acidity values of the Ni-SS1, Ni-SS2, and Ni-SS3 catalysts. This could be due to the uneven distribution of the Ni metal on the surface of the catalysts, causing agglomeration of the Ni metal, and ultimately covering of the active sites on the catalysts. This may have occurred due to the amount of Ni metal dispersed in the catalyst framework. At a lower concentration, Ni particles will be distributed evenly on the catalyst surface. If the amount of metal carried is excessive, it can cause metal sintering that can cover most of the pores of the catalyst [19]. Thus, the impregnation of the Ni metal, which should contribute to the acid sites, would not be performed optimally.

2.3. XRD Analysis of Catalysts

The diffractograms for all of the catalysts are shown in Figure 2. The results showed that all the catalyst samples were amorphous, indicated by the absence of sharp peaks in the diffractograms [28]. All the XRD patterns of the catalysts showed a broad and large peak at 2θ of approximately 22° . The resulting peaks, according to the JCPDS 39-1425, indicated that the silica catalyst had been successfully formed. Figure 2 also shows that activation with sulfuric acid did not change the crystal structure of the SiO₂ material, as the two diffractograms appear similar. A decrease in the peak intensity, caused by the sulfate ions that successfully entered the SiO₂ catalyst framework, could be observed in the diffractograms of the SiO₂ and SS catalysts.

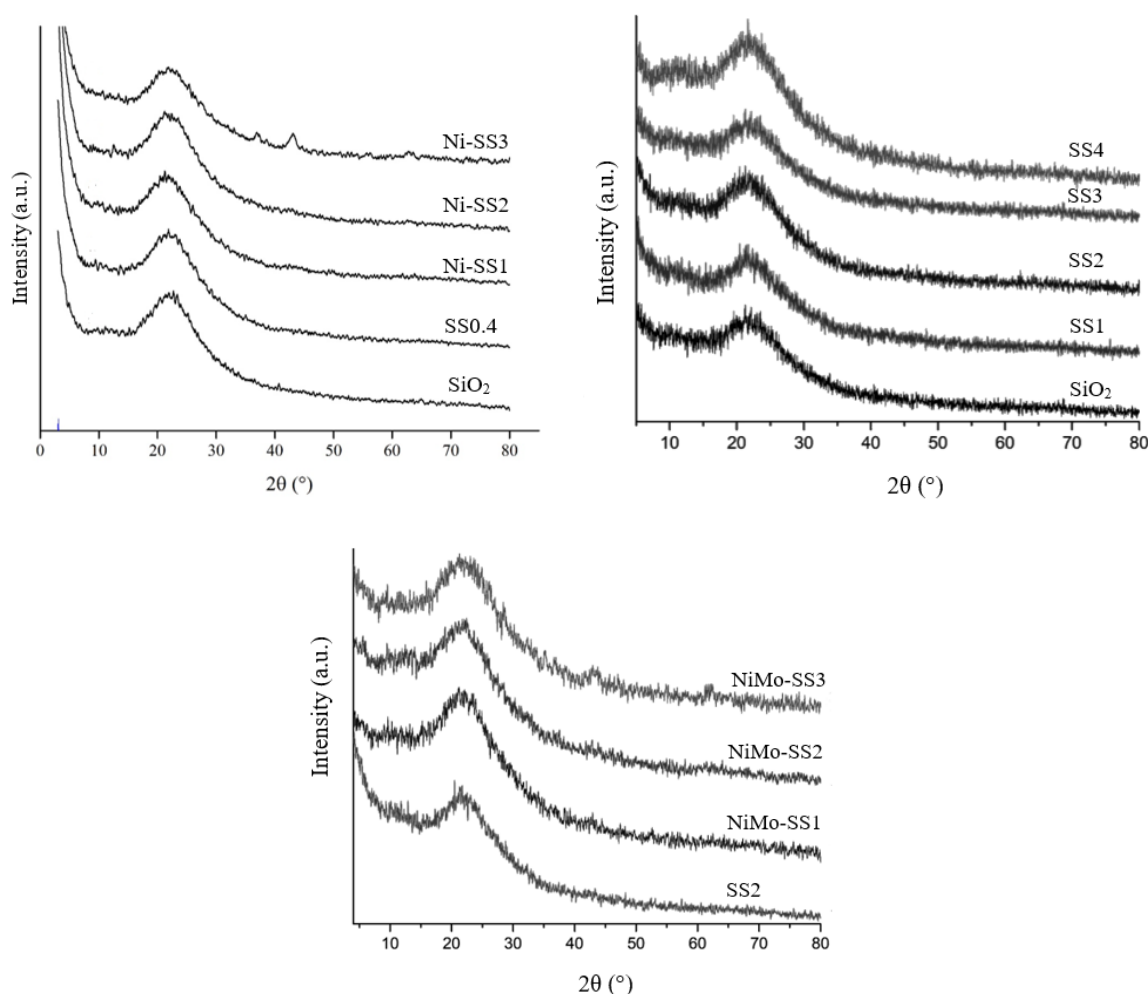


Figure 2. XRD pattern of all catalysts.

The diffractograms of the Ni-SS1, Ni-SS2, and Ni-SS3 catalysts did not show the typical Ni peaks that would be expected to appear, according to JCPDS 04-0850, at 2θ of 44.51° , 51.85° , and 76.37° . This could be due to the low concentration of Ni metal present on the SS0.4 catalyst matrix, rendering it below the detection limit of the XRD instrument.

Nevertheless, the impregnation process of Ni and Mo metals for NiMo/SS was successfully carried out. This is demonstrated by the presence of Mo metal, indicated by peaks in the areas around 12.3° , 23.3° , 26.0° , 39.1° , and 53.8° (JCPDS 01-081-067). The Ni metal is indicated by the appearance of peaks in the regions of 44.5° , 51.8° , and 76.3° , according to JCPDS 04-0850. The peaks observed signify that the silica structure remained amorphous, and that there was no change in the silica structure with the addition of the Ni and Mo metals.

2.4. Scanning Electron Microscope-Energy Dispersive X-ray (SEM-EDX) Analysis

The microstructure analysis of SiO_2 and SS0.4 catalysts is shown by the SEM images in Figure 3. The SEM images of the catalysts show that the particle size was not uniform, consisting of clusters that appeared to look like flakes with clear boundaries. The SEM images of the SS0.4 catalyst show the presence of particle agglomeration with irregular shapes on the surface of the catalyst, which was an indication of the successful addition of sulfate ions. Additionally, the SEM images of the SS0.4 catalyst appeared to be brighter compared to that of the SiO_2 catalyst, which can be attributed to the presence of highly charged ions, specifically SO_4^{2-} [29].

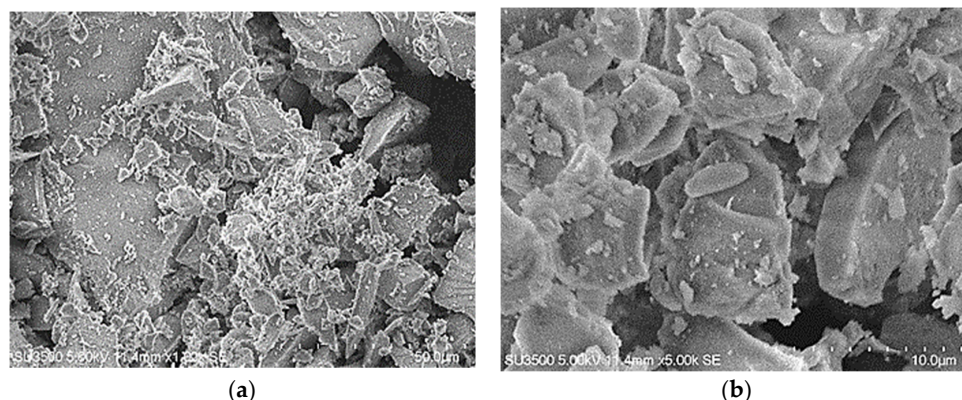


Figure 3. SEM images of (a) SiO₂ and (b) SS0.4 catalyst at 5000× magnifications.

The elemental composition analysis of SiO₂, SS0.4, and Ni-SS1 catalysts is shown in Table 2. The EDX analysis revealed an increase in the S and O content in the SS and Ni-SS1 catalysts, indicating that the sulfate ions had been successfully incorporated onto the SiO₂ catalyst matrix. Moreover, the concentration of Ni metal in the Ni-SS1 catalyst was only 0.5 wt% based on the EDX characterization. This may have occurred because of the competition for metal interaction on the SS0.4 catalyst support. This data is in agreement with a previous study by Amin et al. [19]. Based on the EDX data, unexpectedly, the SiO₂ and SS0.4 catalysts contained a small percentage of Ni metal (0.3%). This was probably due to the presence of Ni atom impurities on the SEM-EDX test plate.

Table 2. EDX of the elements present in the catalysts.

Sample	Mass of Element (%)				
	Si	O	S	Ni	Mo
Ni/SS catalyst	-	-	-	-	-
SiO ₂	17.5	63.3	1.5	0.3	-
SS0.4	20.3	64.6	2.1	0.3	-
Ni-SS1	23.7	72.5	3.2	0.5	-
NiMo/SS catalyst	-	-	-	-	-
SiO ₂	24.09	75.91	-	-	-
NiMo-SS3	14.84	60.88	3.15	6.23	2.91

The morphologies of the SiO₂ and NiMo-SS3 catalysts at 10,000× magnifications are shown in Figure 4. The SEM image of SiO₂ presented in Figure 4a shows that the SiO₂ appears like chunks. After the addition of sulfuric acid and NiMo metals (Figure 4b), the presence of agglomerated particles of irregular size was confirmed. The presence of SO₄²⁻ ions on the surface of the SiO₂ caused the morphology of NiMo-SS3 to appear brighter than SiO₂ [28]. This indicates that the sulfate group had been successfully impregnated on the SiO₂ surface. This data is in agreement with the elemental composition analysis presented in Table 2.

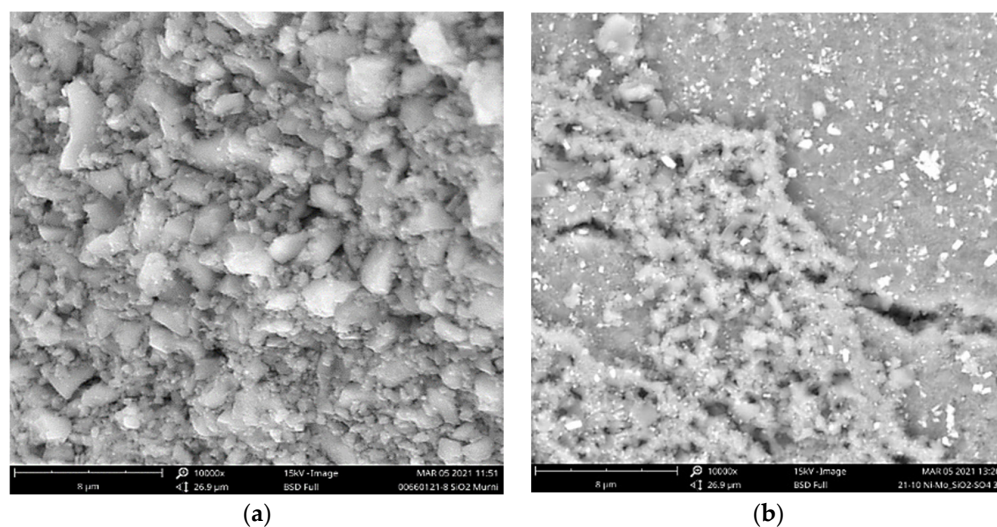


Figure 4. SEM images of (a) SiO₂ and (b) NiMo-SS3 at 10,000× magnifications.

Table 2 shows the distribution data of the elements on the SiO₂ and NiMo-SS3 catalysts. In the EDS data, the S element has appeared on the NiMo-SS3 catalyst indicating that the sulfate ion had been successfully impregnated on the SiO₂ catalyst. There is a reduction in the mass of the O element in the NiMo-SS3 catalyst. This phenomenon could have happened due to the leaching or loss of sulfate groups from the surface of sulfated silica during the nickel impregnation. The amount of the Ni metal that was impregnated in the preparation of the catalyst was 3 wt%, but from the EDX data, the concentration of Ni metal observed was 6.23%. The difference in concentration could also be due to the uneven distribution of the metal. Such a distribution could have created focused clusters of the metal at certain points that, when analyzed, resulted in the higher observed concentration. The Mo metal was impregnated at a concentration of 3%. The EDS data showed a Mo metal concentration in the NiMo-SS 3 catalyst of 2.91%. The difference of 0.09% can be accounted for by the less-than-optimal impregnation process, resulting in a different percentage of element mass.

2.5. Thermogravimetry and Differential Scanning Calorimetry (TG/DSC) Analysis

Based on the TGA/DSC curves of SiO₂ shown in Figure 5, the first mass loss of 4.85% at 165 °C can be attributed to the evaporation of water from the sample, as indicated by the endothermic peak on the DSC curve. In the temperature range of 400–1000 °C, an endothermic event occurred with a second mass loss of 5.54%, indicating that the sample was dominated by water molecules that were bound to Si-OH [29]. The mass reduction at above 1000 °C occurred in only a very small portion, indicating a little decomposition. At that temperature, the sample had begun to stabilize.

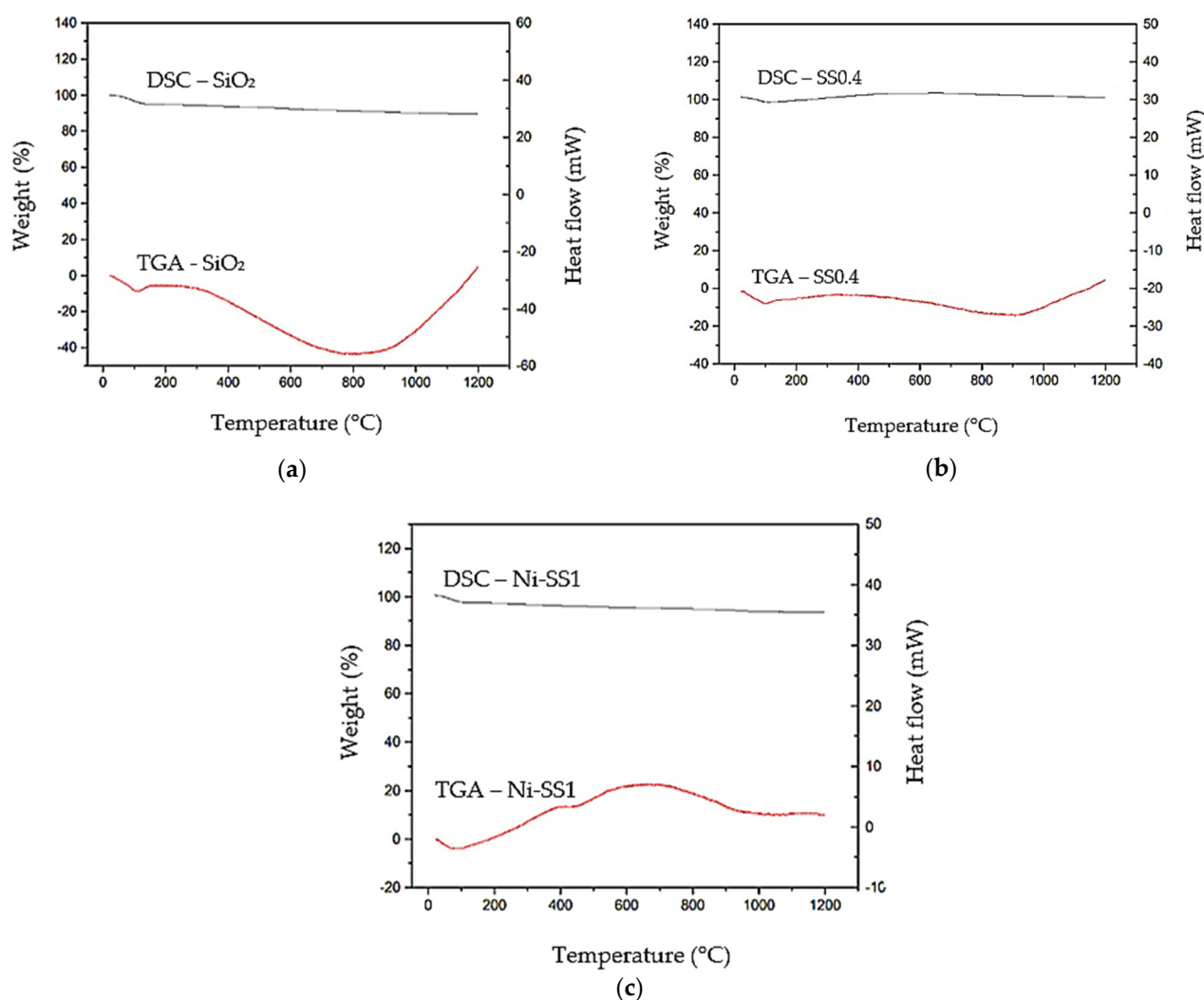


Figure 5. TG/DSC thermograms of (a) SiO₂, (b) SS0.4, and (c) Ni-SS1 catalysts.

The TGA curve of the SS0.4 catalyst shows that the mass reduction of 2.42% at 114 °C corresponded to the occurrence of sample dehydration, with the endothermic loss of H₂O molecules from the sample. In the temperature range of 144–632 °C, there is an exothermic peak which indicates the recrystallization process associated with changes in the material structure [30]. There was also a mass reduction of ~2.65% between 635 and 1200 °C, indicated by the presence of an endothermic peak that can be attributed to the decomposition of sulfate ions on the catalyst material [31]. In the TGA of the Ni-SS1 catalyst, there was a mass reduction of 2.85% in the temperature range of 43–171 °C with the endothermic release of H₂O molecules from the material. An endotherm was formed in the temperature range of 395–532 °C with a mass reduction of 1.74%, indicating the decomposition of nickel nitrate trapped in the matrix pores [31]. Between 939 and 1173 °C, an endothermic peak was also formed with a mass reduction of 2.21%, indicating the decomposition of sulfate ions bound to the catalyst material [30]. The thermal stability of the catalyst was improved by the sulfation and the impregnation of Ni metal, as indicated by the lesser reduction in mass that occurred.

Figure 6 illustrates the TGA/DSC thermogram of the SS2 catalyst. From the TGA curve of the SS2 catalyst, a mass decrease of 2.71%, and an endothermic peak, shown on the DSC curve, can be observed in the temperature range of 50–200 °C. This mass decrease represents the evaporation process of water molecules that were adsorbed, through an endothermic process. In the temperature range of 500–700 °C, the DSC curves present an

exothermic peak. This peak indicates the decomposition of SO_4^{2-} ions on the surface of the catalyst which caused an increase in the silica crystallinity [32]. In the TGA curve, a mass decrease of 2.75% was observed at a temperature range of 500–1000 °C. The total mass of SS2 catalyst lost was 5.46%.

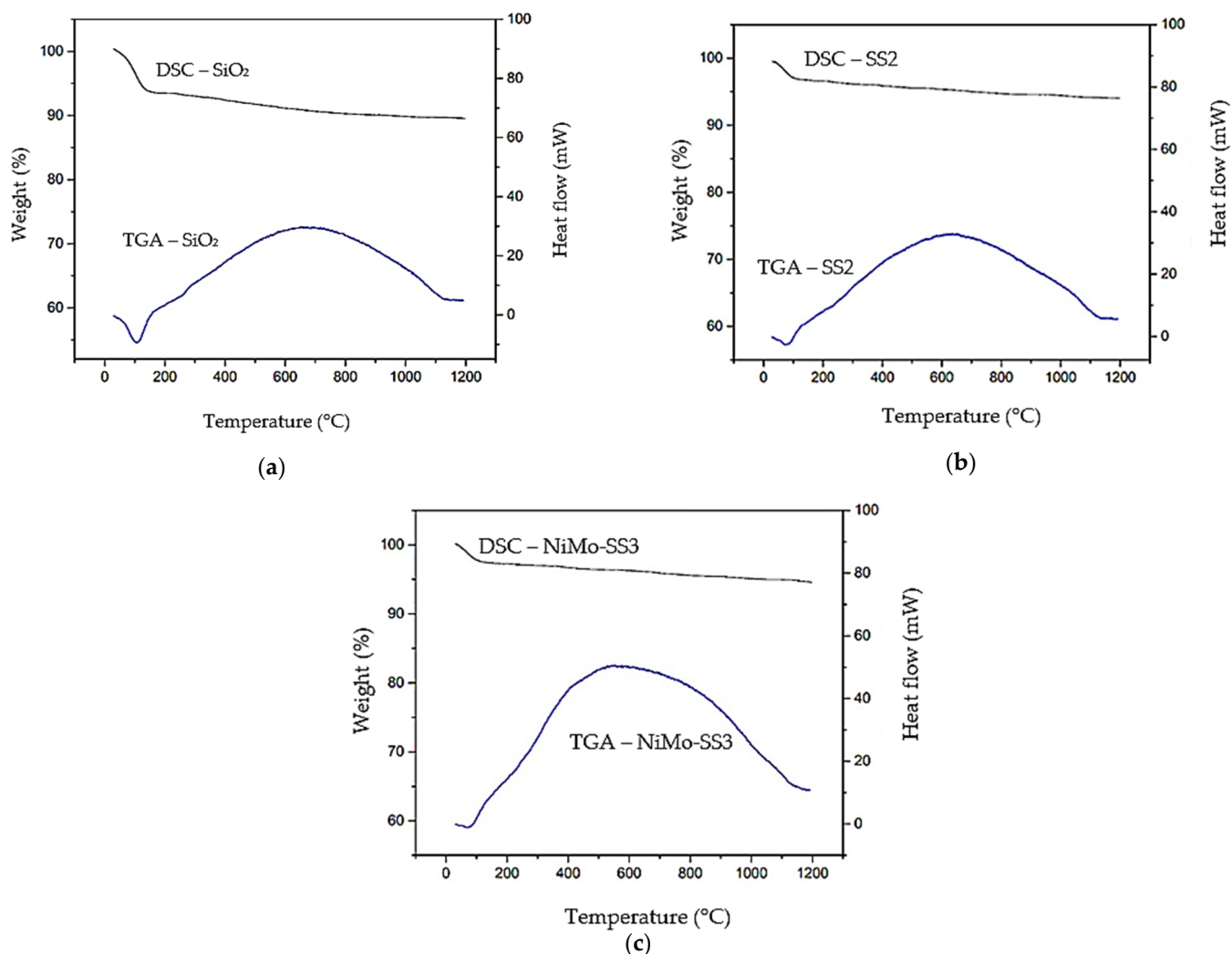


Figure 6. TG/DSC thermograms of (a) SiO_2 , (b) SS2, and (c) NiMo-SS3 catalysts.

Figure 6 also shows the TGA/DSC thermogram of the 3%NiMo- SiO_2/SO_4 (NiMo-SS3) catalyst. The TGA curve shows a mass reduction of 2.62%, accompanied by the presence of an endothermic peak on the DSC curve in the temperature range of 50–150 °C. This mass reduction was due to the release of physically adsorbed water molecules from the catalyst. In the temperature range of 500–800 °C, the DSC curve shows an exothermic peak indicating a change to a more stable structure, with a mass reduction of 2.96%.

2.6. Results for the Hydrocracking Process with Ni/SS Catalysts Using Waste Frying Oil

The performance of the catalysts in the hydrocracking process was evaluated to determine their catalytic activity and selectivity in the conversion of waste frying oil into the gasoline fraction. The catalytic activity was determined by calculating the conversion of the liquid product formed with each catalyst variant, while the catalyst selectivity was determined by analyzing the chemical composition of the liquid product using Gas Chromatography-Mass Spectrometer (GC-MS).

The results of the catalyst activity test are shown in Figure 7. Based on the diagram, the SS0.4 catalyst had the highest catalytic activity with a liquid product yield of 72.47%.

This is because the sulfation process had caused the SS0.4 catalyst to have the highest acidity value. Catalysts with a high acidity value can greatly contribute to the formation of cracking products through the Brønsted and Lewis acid sites on the catalyst. These acid sites play an important role in the hydrogenation process (the cleavage of the double bonds from the reactants) and the formation of reactive carbocations [33]. The Ni-SS2 catalyst also produced a considerable amount of the liquid product, even though the acidity value of the Ni-SS2 was lower than that of the SiO₂ and SS0.4 catalysts. The presence of Ni metal deposited onto the SS catalyst matrix can reduce the presence of carbon or coke deposition in the hydrocracking reaction that can deactivate the catalyst. Ma et al. [34] reported that Ni metal has the ability to break down hydrogen (H₂), allowing it to store hydrogen radicals on the surface of the catalyst that can maximize the hydrocracking reaction. The conversion of the liquid product on the Ni-SS1 catalyst was lower than that of the Ni-SS2 catalyst even though the acidity value of the Ni-SS1 catalyst was higher than that of the Ni-SS2 catalyst. This is due to the high acidity value of the Ni-SS1 catalyst that can, counterproductively, induce the formation of coke, preventing the catalyst from being able to maintain its activity for a longer time. The data on the percentage of coke from each catalyst is shown in Table 3.

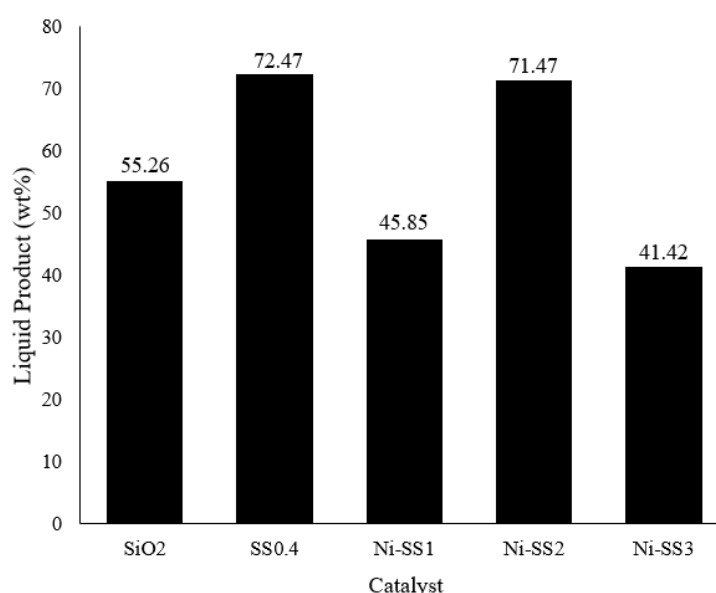


Figure 7. Percentage of the liquid product from the catalytic hydrocracking of waste frying oil at 450 °C with different catalysts.

Table 3. Percentage of coke formed using different catalysts.

Catalyst	Coke (%)
SiO ₂	1.04
SS0.4	0.95
Ni-SS1	0.47
Ni-SS2	-
Ni-SS3	0.43

The resulting liquid products were divided into two: hydrocarbon and non-hydrocarbon products. The non-hydrocarbon liquid products comprised saturated and unsaturated fatty acids that had not been completely cracked in the hydrocracking process, and ketones and alcohol, produced as byproducts of the hydrocracking reaction. The liquid hydrocarbon products consisted of alkanes, alkenes, and cyclic compounds, which were divided into several fractions, including a light fraction (C₁-C₄), a gasoline fraction (C₅-C₁₂), and a diesel fraction (C₁₃-C₂₂). The results of the catalyst selectivity test in the hydrocracking process of

used cooking oil are shown in Table 4. Each catalyst showed a different selectivity towards the liquid product fractions.

Table 4. Catalyst selectivity test from the catalytic hydrocracking of waste frying oil.

Sample	Selectivity (wt%)			
	Light Fraction	Gasoline Fraction	Diesel Fraction	Non-Hydrocarbon Fraction
SiO ₂	-	26.12	2.73	26.41
SS0.4	-	51.71	5.89	14.86
Ni-SS1	-	38.66	1.52	5.68
Ni-SS2	-	58.73	0.39	12.35
Ni-SS3	-	35.93	1.19	4.29

Based on Table 4, the samples were generally more selective towards the gasoline fraction. The Ni-SS2 catalyst exhibited the highest selectivity towards the gasoline fraction with a yield of 58.73%. In contrast, this catalyst had the lowest selectivity towards the diesel fraction, with a yield of only 0.39%. The presence of sulfate and Ni metal can increase the acidity sites, and the resistance of the catalyst to deactivation from carbon residues; thus, it can increase the effective contact between the feed and hydrogen and cause the hydrocracking process to take place more effectively to produce the gasoline fraction. This also applied to the Ni-SS1 and Ni-SS3 catalysts which showed a higher percentage of selectivity for the gasoline fraction than the SiO₂ catalyst, despite the lower acidity values of the Ni-SS1 and Ni-SS3 catalysts. For the SS0.4 and SiO₂ catalysts that were not impregnated with Ni, carbon residue deposition can easily occur on the active site of the catalysts, rendering their catalytic ability to crack oil into the gasoline fraction less than optimal. However, the SS0.4 catalyst showed a high percentage selectivity for the gasoline fraction due to the high acidity value of the SS0.4 catalyst. Again, the higher the acidity of the catalyst, the higher the number of active sites that become cracking reaction mediums.

2.7. Results for the Hydrocracking Process with NiMo/SS Catalysts Using Fresh Frying Oil

Based on Figure 8, SiO₂ had the lowest liquid product conversion, attributed to its low acidity. However, the catalytic activity of SS increased due to the presence of sulfate ions which provided additional active sites for the hydrocracking process. Additionally, the presence of NiMo metals on the catalyst significantly increased the amount of liquid product. The greater the concentration of Ni and Mo, the more liquid product was produced. This concentration is correlated with the acidic properties of the catalysts which increased after metal impregnation.

Table 5 shows the catalytic selectivity for the hydrocracking of fresh frying oil. The results show that all of the catalysts were selective towards the gasoline fraction. The SS catalyst had higher selectivity compared to the SiO₂ catalyst. The highest selectivity towards the gasoline fraction was achieved by the NiMo-SS3 catalyst (43.22 wt%). The acidity properties were related to the catalytic selectivity. Based on the acidity properties, the NiMo-SS1 and NiMo-SS2 catalysts had lower acidity compared to the NiMo-SS3 catalyst, thus producing lower selectivity for the gasoline product (32.05 and 35.44 wt%, respectively).

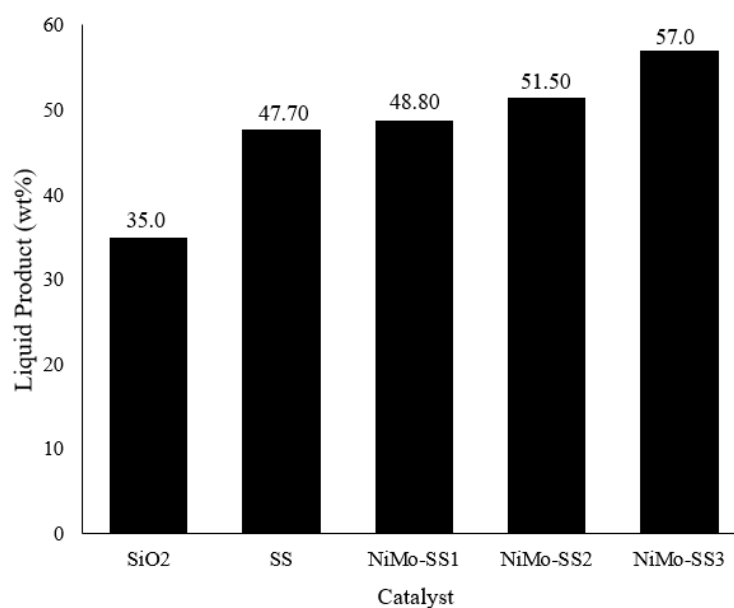


Figure 8. Percentage of the liquid product from the catalytic hydrocracking of fresh frying oil at 450 °C with different catalysts.

Table 5. Catalyst selectivity test from the catalytic hydrocracking of fresh frying oil.

Catalyst	Selectivity (%w/w)			
	Light Fraction	Gasoline Fraction	Diesel Fraction	Non-Hydrocarbon Fraction
SiO ₂	-	23.48	1.01	10.51
SS	-	35.38	0.95	11.38
NiMo-SS1	-	32.05	1.81	14.94
NiMo-SS2	-	35.44	0.47	15.58
NiMo-SS3	0.20	43.22	2.34	11.24

As shown in Table 6, the gasoline fraction from the hydrocracking reaction of waste frying oil over Ni-SS2 was higher compared to that observed by Wijaya et al. [35] using a nickel catalyst supported on sulfated zirconia-pillared bentonite. On the other hand, the NiMo-SS3 catalyst was relatively effective during fraction into gasoline and diesel products compared to Nurmalasari et al. [36]. These results show that the catalyst successfully increased the catalytic selectivity.

Table 6. Comparison data of liquid yield in the hydrocracking reaction.

Parameter	Current Study		Ni/BZS0.5 [35]	NiMo/MS [36]
	Ni-SS2	NiMo-SS3		
Gasoline product (wt%)	58.73	43.22	30.52	9.42
Diesel product (wt%)	0.39	2.34	4.16	33.82

3. Materials and Methods

3.1. Materials

The materials used for silica synthesis were tetraethyl orthosilicate (TEOS), ethanol (C₂H₅OH), methanol (CH₃OH), hydrochloric acid (HCl) 37%, sulfuric acid (H₂SO₄) 98%, and silver nitrate (AgNO₃). Nickel nitrate hexahydrate (Ni(NO₃)₂·6H₂O), nickel chloride hexahydrate (NiCl₂·6H₂O), and ammonium heptamolybdate tetrahydrate ((NH₄)₆Mo₇O₂₄·

4H₂O) were used for the impregnation process. Each chemical was purchased from Merck & Co. Feed was collected from domestic waste for the hydrocracking process.

3.2. Preparation of Ni/SS

The sulfated silica was prepared by the sol-gel method of TEOS, using 30 mL ethanol, and 2.22 mL H₂SO₄ (0.4 M). The mixture was agitated to form a white transparent gel. The gel was then heated for 3 h at 100 °C and refluxed with methanol for 72 h at 80 °C. The samples were dried in an oven and were later calcined at 600 °C for 4 h. The solids were labeled as SS0.4.

The impregnation of Ni metal on the SS catalyst was carried out with 1, 2, and 3 wt% Ni (Ni(NO₃)₂·6H₂O) in 25.3 mL methanol. The solution was stirred for 2 h at room temperature. The remaining solvent was evaporated at 80 °C using an oven, and the catalyst precipitate was dried in the oven at 105 °C for 2 h. The solids were then calcined at 500 °C for 3 h, reduced with hydrogen gas (20 mL/min) at 400 °C for 3 h, and were labeled as Ni-SS1, Ni-SS2 and Ni-SS3.

3.3. Preparation of NiMo/SS

Sulfated silica was synthesized with H₂SO₄ at different concentrations (1, 2, and 3 M). A quantity of 16.8 mL of TEOS, 30 mL H₂SO₄, and 30 mL ethanol was mixed. The mixture was then stirred and heated at 80 °C to form a transparent gel. The gel was dried in an oven at 100 °C, then calcined at 600 °C for 4 h. The catalysts were subsequently labelled SS1, SS2, SS3, and SS4.

The catalyst with the highest acidity was applied to the impregnation process with 1, 2, or 3 wt% of NiCl₂·6H₂O and (NH₄)₆Mo₇O₂₄·4H₂O using distilled water. The solution was stirred for 24 h at room temperature, then evaporated at 80 °C. The precipitate was dried at 100 °C for 3 h. The solid catalyst was calcined at 500 °C for 3 h, then reduced at 400 °C for 3 h with H₂ gas at a flow rate of 20 mL/min. The obtained catalysts were denoted as NiMo-SS1, NiMo-SS2, and NiMo-SS3.

3.4. Hydrocracking Process

The hydrocracking process of fresh and waste frying oil was carried out in a hydrocracking reactor with H₂ gas (flow rate of 20 mL/min) and a catalyst/feed ratio of 1/100. The hydrocracked liquid product was collected and analyzed using GC-MS.

3.5. Catalyst Characterization

The Fourier transform infrared (FTIR) spectra of the catalysts were obtained using FTIR, Shimadzu Prestige-21, Japan in the range of 4000–400 cm⁻¹ with the KBr pellet technique. X-ray diffraction (XRD) analysis was performed using the X'pert Pro PANalytical with a Cu X-Ray tube (1.5406 Å). The acidity test was carried out gravimetrically using ammonia and pyridine adsorption. Scanning electron microscope (SEM) imaging and EDX elemental analysis were performed using High-Tech's scanning electron microscopes (Hitachi) SU 3500 (Japan). Thermogravimetry analysis and differential scanning calorimetry (TGA/DSC) were carried out under air atmosphere with a temperature range of 30–1200 °C (a heating rate of 10 °C/min). Gas chromatography-mass spectrometer (GC-MS) analysis of the hydrocracked liquid products was carried out using Shimadzu QP2010S (Japan) with the RTx-5MS chromatography column, column length of 30 m, helium carrier gas, and EI 70 eV.

4. Conclusions

The synthesis of sulfated silica using the sol-gel method and its modification using Ni metal by the wet impregnation method were successfully carried out. Ni and/or Mo impregnated on sulfated silica was used for the hydrocracking reaction using fresh and waste frying oil. Among the catalysts investigated, Ni-SS2 exhibited the best performance for the hydrocracking reaction over waste frying oil. This catalyst was able to achieve a

conversion of the liquid product of 71.47% and a selectivity of 58.73% for the gasoline fraction. NiMo-SS3 showed the best percentage of activity and selectivity in the hydrocracking of fresh frying oil at 51.50 and 43.22 wt%, respectively. Although the acidity value is directly proportional to the catalysts' ability, it is not the sole factor that determines conversion yield. In particular, it is necessary to optimize the ratio of catalyst to feed in the hydrocracking process.

Author Contributions: Conceptualization, K.W.; methodology, K.W.; validation, K.W.; formal analysis, A.D. and A.F.P.; investigation, A.D. and A.F.P.; resources, K.W.; data curation, A.N. and A.C.W.; writing—original draft preparation, A.D. and A.F.P.; writing—review and editing, K.W.; A.N.; and A.D.T.; supervision, K.W.; funding acquisition, K.W. All authors have read and agreed to the published version of the manuscript.

Funding: This research was supported and funded by World Class Research (WCR) 2021.

Conflicts of Interest: The authors declare no conflict of interest.

References

1. Utami, M.; Wijaya, K.; Trisunaryanti, W. Pt-promoted sulfated zirconia as catalyst for hydrocracking of LDPE plastic waste into liquid fuels. *Mater. Chem. Phys.* **2018**, *213*, 548–555. [[CrossRef](#)]
2. Dandik, L.; Aksoy, H.A. Pyrolysis of used sunflower oil in the presence of sodium carbonate by using fractionating pyrolysis reactor. *Fuel Process. Technol.* **1998**, *57*, 81–92. [[CrossRef](#)]
3. Lotero, E.; Liu, Y.; Lopez, D.E.; Suwannakarn, K.; Bruce, D.A.; Goodwin, J.G. Synthesis of biodiesel via acid catalysis. *Ind. Eng. Chem. Res.* **2005**, *44*, 5353–5363. [[CrossRef](#)]
4. Burda, C.; Chen, X.; Narayanan, R.; El-Sayed, M.A. Chemistry and properties of nanocrystals of different shapes. *Chem. Rev.* **2005**, *105*, 1025–1102. [[CrossRef](#)] [[PubMed](#)]
5. Olindo, R.; Li, X.; Lercher, J.A. Activation of light alkanes on sulfated zirconia. *Chem. Ing. Tech.* **2006**, *78*, 1053–1060. [[CrossRef](#)]
6. Hauli, L.; Wijaya, K.; Syoufian, A. Fuel production from ldpe-based plastic waste over chromium supported on sulfated zirconia. *Indones. J. Chem.* **2019**, *20*, 422–429. [[CrossRef](#)]
7. Bergna, H.E.; Roberts, W.O. Colloidal silica: Fundamentals and applications. *Mech. Eng. J.* **2006**, *22*, 9–37. [[CrossRef](#)]
8. Lai, C.Y. Mesoporous silica nanomaterials applications in catalysis. *J. Thermodyn. Catal.* **2013**, *5*, 1–3. [[CrossRef](#)]
9. Luo, T.Y.; Liang, T.X.; Li, C.S. Stabilization of cubic zirconia by carbon nanotubes. *Mater. Sci. Eng. A* **2004**, *366*, 206–209. [[CrossRef](#)]
10. Radwan, N.R.; Hagar, M.; Afifi, T.H.; Al-wadaani, F.; Okasha, R.M. Catalytic activity of sulfated and phosphated catalysts towards the synthesis of substituted coumarin. *Catalysts* **2018**, *8*, 36. [[CrossRef](#)]
11. Pooyan, S.S. Sol-gel process and its application in nanotechnology. *J. Polym. Eng. Technol.* **2005**, *13*, 38–41.
12. Usi, E.P.S.; Wijaya, K.; Wangsa; Pratika, R.A.; Hariani, P.L. Effect of nickel concentration in natural zeolite as catalyst in hydrocracking process of used cooking oil. *Asian J. Chem.* **2020**, *32*, 2773–2777. [[CrossRef](#)]
13. Wijaya, K.; Baobalaguna, G.; Trisunaryanti, W.; Syoufian, A. Hydrocracking of palm oil into biogasoline catalyst by Cr/natural zeolite. *Asian J. Chem.* **2013**, *25*, 8981–8986. [[CrossRef](#)]
14. Izumi, Y.K.; Hisano, K.; Hida, T. Acid catalysis of silica-included heteropolyacid in polar reaction media. *Appl. Catal. A Gen.* **1999**, *181*, 277–282. [[CrossRef](#)]
15. Chavan, F.B.; Madje, J.; Bharad, M.; Ubale, M.; Ware, S.; Hinde, N. Silica gel supported NaHSO₄ catalyzed organic reaction: An efficient synthesis of coumarins. *Bull. Catal. Soc. India* **2008**, *7*, 41–45. [[CrossRef](#)]
16. Clearfield, A.; Serrette, G.P.D.; Khazi-Syed, A.H. Nature of hydrous zirconia and sulfated hydrous zirconia. *Catal. Today* **1994**, *20*, 295–312. [[CrossRef](#)]
17. Fu, B.; Gao, L.; Nia, L.; Wei, R.; Xiao, G. Biodiesel from waste cooking oil via heterogeneous superacid catalyst SO₄²⁻/ZrO₂. *Energ. Fuel* **2009**, *23*, 569–572. [[CrossRef](#)]
18. Augustine, J.R. *Heterogeneous Catalysis for the Synthetic Hemist*, 1st ed.; Marcel Decker, Inc.: New York, NY, USA, 1990. [[CrossRef](#)]
19. Amin, A.K.; Wijaya, K.; Trisunaryanti, W. The catalytic performance of ZrO₂-SO₄ and Ni/ZrO₂-SO₄ Prepared from Commercial ZrO₂ in hydrocracking of LDPE plastic waste into liquid fuels. *Orient. J. Chem.* **2018**, *34*, 3070. [[CrossRef](#)]
20. Sriningsih, W.; Saerodji, M.G.; Trisunaryanti, W.; Armunanto, R.; Falah, I.I. Fuel production from LDPE plastic waste over natural zeolite supported Ni, Ni-Mo, Co and Co-Mo metals. *Procedia Environ. Sci.* **2014**, *20*, 215–224. [[CrossRef](#)]
21. Garcia, C.M.; Teixeira, S.; Marciniuk, L.L.; Schuchardt, U. Transesterification of soybean oil catalyzed by sulfated zirconia. *Bioresource Technol.* **2008**, *99*, 6608–6613. [[CrossRef](#)] [[PubMed](#)]
22. Wijaya, K.; Saputri, W.D.; Aziz, I.T.A.; Herald, E.; Hakim, L.; Suseno, A.; Utami, M. Mesoporous silica preparation using sodium bicarbonate as template and application of the silica for hydrocracking of used cooking oil into biofuel. *Silicon* **2021**, 1–9. [[CrossRef](#)]
23. Ghoreishi, K.B.; Yarmo, M.A. Sol-gel sulfated silica as a catalyst for glycerol acetylation with acetic acid. *J. Sci. Tech.* **2013**, 65–78.

24. Tyagi, B.; Mishra, M.K.; Jasra, R.V. Solvent free synthesis of acetyl salisilic acid over nano-crystalline sulfated. *J. Mol. Catal. A-Chem.* **2010**, *317*, 41–45. [[CrossRef](#)]
25. Trisunaryanti, W.; Wijaya, K.; Triyono, T.; Adriani, A.R.; Larasati, S. Green synthesis of hierarchical porous carbon prepared from coconut lumber sawdust as Ni-based catalyst support for hydrotreating Callophyllum inophyllum oil. *Results Eng.* **2021**, *11*, 100258. [[CrossRef](#)]
26. Hanifa, A.; Nadia, A.; Saputri, W.D.; Syoufian, A.; Wijaya, K. Performance of Ni-Mo Sulfated Nanozirconia Catalyst for Conversion of Waste Cooking Oil into Biofuel via Hydrocracking Process. *Mater. Sci. Forum* **2021**, *1045*, 79–89. [[CrossRef](#)]
27. Ahmed, A.I.; El-Hakam, S.A.; Samra, S.E.; EL-Khouly, A.A.; Khder, A.S. Structural characterization of sulfated zirconia and their catalytic activity in dehydration of ethanol. *Colloids Surf. A Physicochem. Eng. Asp.* **2008**, *317*, 62–70. [[CrossRef](#)]
28. Patel, A.; Brahmkhatri, V.; Singh, N. Biodiesel production by esterification of free fatty acid over sulfated zirconia. *Renew. Energy* **2013**, *51*, 227–233. [[CrossRef](#)]
29. Saber, O.; Gobara, H.M. Optimization of Silica Content in Alumina-Silica Nanocomposites to Achieve High Catalytic Dehydrogenation Activity of Supported Pt Catalyst. *Egypt. J. Pet.* **2014**, *23*, 445–454. [[CrossRef](#)]
30. Tizzoni, A.C.; Corsaro, N.; D'Ottavi, C.; Licocchia, S.; Sau, S.; Tarquini, P. Oxygen Production by Intermediate Metal Sulphates in Sulphur Based Thermochemical Water Splitting Cycles. *Int. J. Hydrogen Energy* **2015**, *40*, 4065–4083. [[CrossRef](#)]
31. Zangouei, M.; Moghaddam, A.Z.; Arasteh, M. The Influence of Nickel Loading on Reducibility of NiO/Al₂O₃ Catalysts Synthesized by Sol-Gel Method. *Chem. Eng. Res. Bull.* **2010**, *14*, 97–102. [[CrossRef](#)]
32. Sembiring, S.; Simanjuntak, W. X-ray Diffraction Phase Analysis of Mullite Derived from Rice Husk. *Makara J. Sci.* **2012**, *16*, 77–82.
33. Utami, M.; Trisunaryanti, W.; Shida, K.; Tsushida, M.; Kawakita, H.; Ohto, K.; Wijaya, K.; Taminaga, M. Hydrothermal preparation of a platinum loaded sulphated nanozirconia catalyst for the effective conversion of waste low density polyethylene into gasoline-range hydrocarbons. *RSC Adv.* **2019**, *9*, 41392–41401. [[CrossRef](#)]
34. Ma, Z.; Meng, X.; Liu, N.; Shi, L. Pd-Ni Doped Sulfated Zirconia: Study of hydrogen spillover and isomerization of n-Hexane. *J. Mol.* **2018**, *449*, 114–121. [[CrossRef](#)]
35. Wijaya, K.; Kurniawan, M.A.; Saputri, W.D.; Trisunaryanti, W.; Mirzan, M.; Hariani, P.L.; Tikoalu, A.D. Synthesis of nickel catalyst supported on ZrO₂/SO₄ pillared bentonite and its application for conversion of coconut oil into gasoline via hydrocracking process. *J. Environ. Chem. Eng.* **2021**, *9*, 105399. [[CrossRef](#)]
36. Nurmalasari, W.T.; Sutarno, I.I.F. Mesoporous Silica Impregnated by Ni and NiMo as Catalysts for Hydrocracking of Waste Lubricant. *Int. J. Chem. Tech. Res.* **2016**, *9*, 607–614.